Front. Earth Sci. 2015, 9(4): 637–641
DOI 10.1007/s11707-015-0515-6

RESEARCH ARTICLE

Modeling of oil spill beaching along the coast of the Bohai Sea, China

Qing XU[1,2,3], Yongcun CHENG (✉)[3,4], Bingqing LIU[5], Yongliang WEI[5]

1 Key Laboratory of Coastal Disasters and Defense of Ministry of Education, Hohai University, Nanjing 210098, China
2 College of Harbor, Coastal and Offshore Engineering, Hohai University, Nanjing 210098, China
3 Center for Coastal Physical Oceanography, Old Dominion University, Norfolk, VA 23529, USA
4 School of Marine Sciences, Nanjing University of Information Science and Technology, Nanjing 210044, China
5 College of Marine Sciences, Shanghai Ocean University, Shanghai 201306, China

Abstract On June 4 and 17, 2011, two separate oil spill accidents occurred at platforms B and C of the Penglai 19-3 oilfield located in the Bohai Sea, China. Based on the initial oil spill locations detected from the first available Synthetic Aperture Radar (SAR) image acquired on June 11, 2011, we performed a numerical experiment to simulate the potential oil spill beaching area with the General NOAA Operational Modeling Environment (GNOME) model. The model was driven by ocean surface currents from an operational ocean model (Navy Coastal Ocean Model) and surface winds from operational scatterometer measurements (the Advanced Scatterometer). Under the forcing of wind and ocean currents, some of the oil spills reached land along the coast of Qinhuangdao within 12 days. The results also demonstrate that the ocean currents are likely to carry the remaining oil spills along the Bohai coast towards the northeast. The predicted oil spill beaching area was verified by reported *in-situ* measurements and former studies based on MODIS observations.

Keywords oil spill, Bohai Sea, trajectory, GNOME, SAR

1 Introduction

Marine oil spills can cause serious damage to fisheries and wildlife, and can negatively impact human activities, especially in coastal regions. Therefore, oil spill monitoring and trajectory simulation have become one of the most important applications for operational oceanography (Hackett et al., 2009; Xu et al., 2010).

Received October 20, 2014; accepted January 12, 2015

E-mail: yccheng.en@gmail.com

Two separated oil spill accidents occurred on June 4 and 17, 2011 at platform B and C of the Penglai 19-3 oilfield in the Bohai Sea, China (Fig. 1). They were the first large-scale oil spill events ever to occur in the China Seas, and were a result from abnormal chlorophyll concentration distributions and red tide nearby the oil spill areas (Guo et al., 2013). Due to the very limited self-purification ability and vulnerability of the coastal zones in the Bohai Sea, many studies focusing on the oil spill events have been carried out in this area (e.g., Sun et al., 2011; Guo et al., 2013; Xu et al., 2013).

Satellite optical (e.g., Moderate Resolution Imaging Spectro-radiometer [MODIS]) and microwave (e.g., Synthetic Aperture Radar [SAR]) instruments have proven to be valuable tools for oil spill monitoring. Single or multi-satellite remote sensing data have been widely used to investigate marine oil spill events in various regions (Hu et al., 2003, 2009; Migliaccio et al., 2007, 2012; Solberg et al., 2007; Ferraro et al., 2009; Garcia-Pineda et al., 2009; Liu et al., 2011; Zhang et al., 2011; Li et al., 2013). However, utilization of satellite remote sensing data for observing oil spill trajectories is limited by the satellite revisit time and the swath. Successive images with high temporal resolution and large spatial coverage are needed. For example, Cheng et al. (2014) used COSMO-SkyMed X-Band SAR images to monitor the largest oil spill accident in the United Kingdom waters in the last decade with a SAR revisit time from 11 hrs to 3 days. However, the oil spill movement still cannot be predicted by using only satellite data. The typical process for tracking oil spill trajectories is by implementing ocean drift models. Among these models, General NOAA Operational Modeling Environment (GNOME) has been widely used due to its easy implementation (Cheng et al. 2011, 2014; Farzingohar et al., 2011; Remyalekshmi and Hegde, 2013). A case in point, Xu et al. (2013) investigated the Bohai Sea oil

spill trajectories using GNOME and combined SAR, MODIS, and Chinese HJ-1-B CCD images.

However, few studies use the drift model to focus on the oil spill beaching risk assessment in the vulnerable coastal zones. As the successive study of Xu et al. (2013), this paper uses GNOME to study the possibilities of simulating the potential oil spill beaching area during the Bohai Sea oil spill events. The model setting and data that are needed to drive the model are described in Section 2. Simulation results are given in Section 3 and the summary is found in Section 4.

2 Model setting and data

GNOME was developed by NOAA/ERD (Emergency Response Division) as a nowcast/forecast model primarily in pollution transport analyses. In GNOME, a volume of spilled oil is denoted as a 'splot' and modeled as Lagrangian Elements (LEs). The model is driven by ocean surface wind and current (Beegle-Krause, 2003, 2005). Each splot represents a portion of the spilled oil. A collective group of splots represents the distribution of spilled oil at a given time. The GNOME model, openly available from NOAA, can calculate both 'best guess trajectories' (Best Guess Solution, BGS) and Minimum Regret Solution (MRS, related to the wind and current uncertainties) and can be implemented with wind/current obtained from other sources in diagnostic mode.

In this study, we obtained the 3-hourly ocean surface current field from the Navy Coastal Ocean Model (NCOM) outputs (Martin et al., 2009) at a spatial resolution of 1/8°× 1/8° (about 14 km×8 km in latitude and longitude). The ocean current data from 00:00 UTC on June 4, 2011 (the beginning date of the oil leak) to 00:00 UTC on June 23, 2011 were continuously updated during the GNOME model run. The study area is 37°N–41°N, 117.5°E – 122.5°E (Fig. 1).

The daily surface wind speed fields from the advanced scatterometer (ASCAT), onboard the meteorological operational platform (MetOp) satellite, were used to drive the GNOME. The ASCAT sea surface wind product is a one-day composite product with a spatial resolution of 0.25°×0.25° (http://coastwatch.pfeg.noaa.gov/). The daily ASCAT wind products in the Bohai Sea are homogenous in the central area of the region. Due to the inaccuracy of the scatterometer wind data near the coastline, a result of land contamination from the radar backscatter signal from the large scatterometer footprint and the complexity of air-sea interaction processes in the coastal waters (Yang et al., 2011), the regional average of the wind field is calculated and the missing data are filled by the spline method. Figure 2 shows the time series of the sea surface wind vectors from 12:00 UTC on June 4 to 12:00 UTC on June 24. It can be seen that the northwest wind of 4–5 $m \cdot s^{-1}$ is dominant during the simulation period. Ocean surface winds can also be retrieved from SAR imagery (Wackerman et al., 2002; Li et al., 2007; Xu et al., 2010). However, SAR does not provide time series of wind measurements.

During the Bohai Sea oil spill events, we collected seven satellite images from ENVISAT ASAR (advanced SAR), MODIS, and Chinese HJ-1-B CCD (see Xu et al., 2013 for more detail). Figure 3 shows the first available ENVISAT ASAR image. The black areas are caused by the oil spill and the white dots are positions of oil platforms and ships that can be extracted from the SAR image using existing target detection algorithm (Wang et al., 2008). The initial distributions of oil spill locations detected from this image

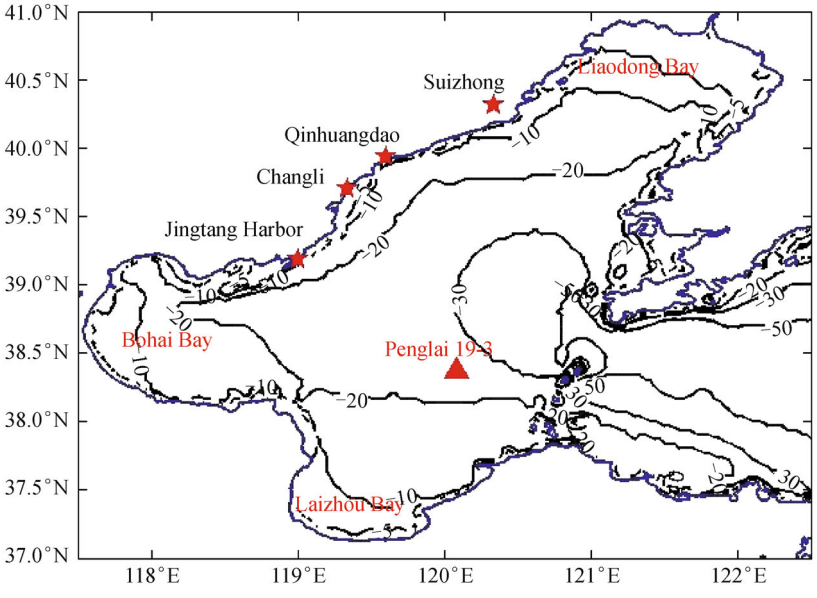

Fig. 1 Bathymetric map of Bohai Sea and location of the Penglai 19-3 oilfield (shown as triangle).

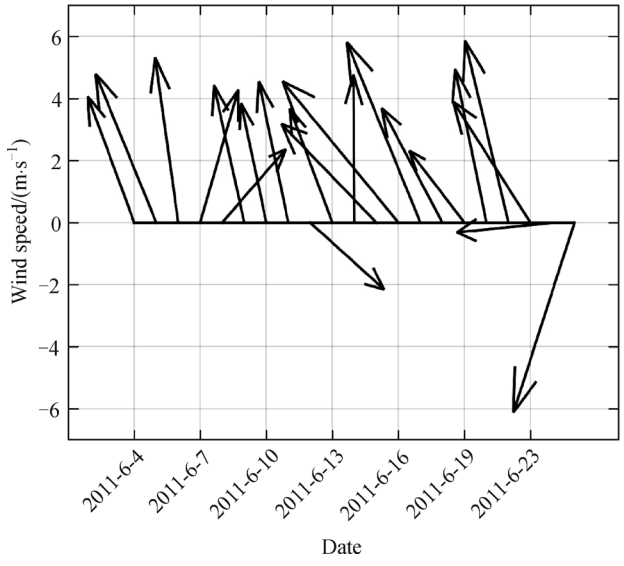

Fig. 2 Surface wind conditions forcing the GNOME model in the Bohai Sea during June 4 to June 23, 2011.

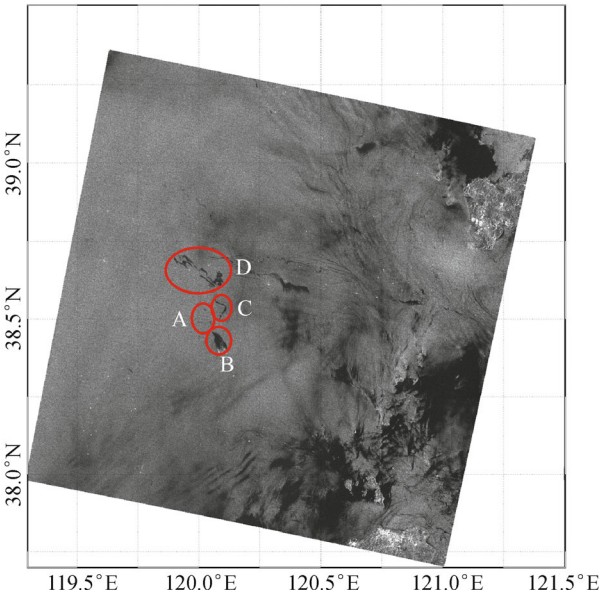

Fig. 3 ENVISAT ASAR image of oil spills in the Bohai Sea acquired at 02:14:57 UTC on June 11, 2011. The observed oil slicks are marked with A–D (after Xu et al., 2013).

are denoted by 'splots' and used as inputs to the GNOME model. The simulation was performed at one hr intervals. A reported amount of 400 barrels of a medium crude oil type was used (based on SAR images and denoted by 500 'splots' to keep the splot mass balance; see Xu et al., 2013) and was released at the ENVISAT ASAR imaging time (i.e., the over flight time in GNOME is 02:14:57 UTC on June 11, 2011).

3 Results and discussion

To assess the risk of oil spill pollution, we run the model until 12:00 UTC, June 22, with ocean current and wind fields from NCOM and ASCAT, respectively. Figure 4

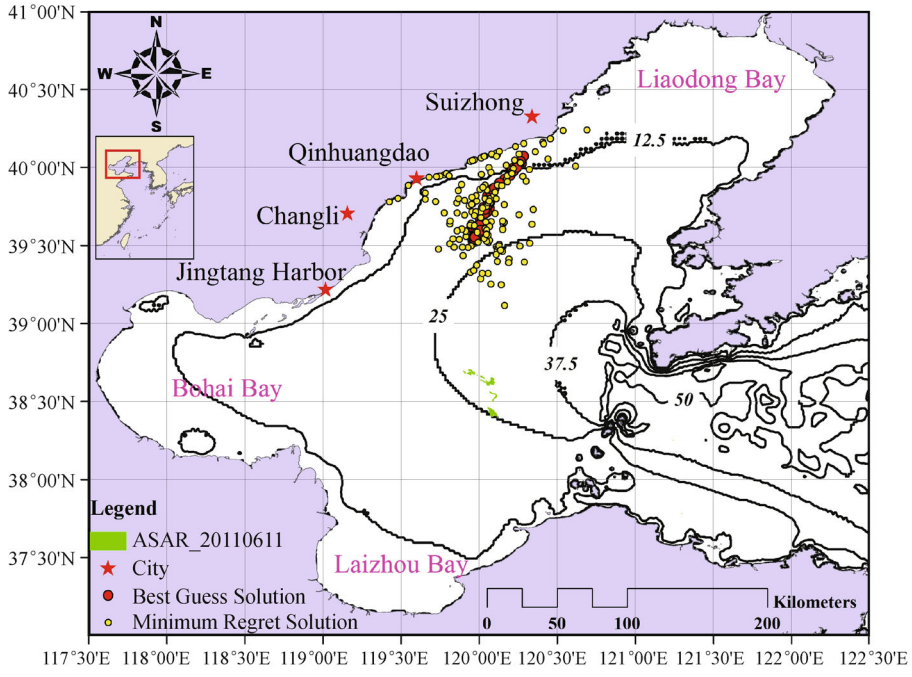

Fig. 4 The distribution of the Best Guess Solution and Minimum Regret Solution splots at 12:00 UTC on June 22, 2011.

shows distribution of the BGS and MRS splots at 12:00 UTC on June 22. The regions covered with the splots denote the distribution of simulated oil slicks. The data also reveal the high risk regions that will be affected by the oil slicks. In Fig. 4, the green regions denote the observed oil spills on the ENVISAT ASAR image on June 11, the initial input to the model simulation. Comparisons of the SAR observations with the locations of the simulated BGS show that the oil spills moved 133 km northward in 12 days. The weathering behaviors of different pollutants are critical to predicting their trajectories. GNOME uses a simple weathering model. Over time, part of the oil evaporates and part of it disperses into the water, so that less and less of the oil remains on the surface. The remaining surface oil also physically changes over time (GNOME manual, http://response.restoration.noaa.gov/sites/default/files/GNOME_Manual.pdf). In this experiment, approximately 59% of the oil splots remained and 41% of the oil slicks disappeared or evaporated during the movement.

The simulation results also demonstrate that the oil may have an impact on the coast between 39°30′N and 40°N on June 22. Due to the wind and relatively stronger currents along the coast of Qinhuangdao (Hebei Province), some pollutants approached land while the remaining pollutants moved northeast along the coastline. The coastal area of Qinhuangdao and Liaodong Bay is at highest risk for oil spill pollution due to these oil spill events. Further, field measurements (e.g., from water samples) are both valuable and necessary for validation.

We do not have an *in-situ* oil spill beaching measurement. However, the existence of sporadic oils in this potential beaching area was validated by later reports from the State Oceanic Administration of China. Figures 5(a) and 5(b) are photos of the oil slicks on the beach in Hebei Province. The regions are consistent with the simulated high risk area of oil slick pollution.

We further compared the model results with the MODIS observations in Guo et al. (2013). Their Fig. 6(a) shows abnormally high chlorophyll concentration distributions along the coast between Jingtang Harbor and Qinhuangdao, and also in regions near the oil leak platforms on June 24, 2011. The MODIS observation shows good agreement with our simulated potential oil spill beaching area shown in Fig. 4. As pointed out by Guo et al. (2013), the plankton, fish eggs, Parr, and shellfish are vulnerable to oil spill pollution. They are particularly sensitive to toxic effects of oil, even at lower oil concentrations. Moreover, the oil film on the sea surface affects phytoplankton photosynthesis by obscuring the sun, making it difficult for the plankton-eating marine life to survive. Once the plankton is contaminated, other advanced species in the food chain are threatened due to bioaccumulation of pollution, resultant high chlorophyll concentration, and red tide over the oil polluted regions. Based on the simulations of Xu et al. (2013), another oil spill event, which occurred on June 17, is related to the abnormally high chlorophyll concentration near the Jingtang Harbor. As shown in Figs. 7 and 8 of Guo et al. (2013), the extents of the oil spill related to the red tide during July and August in the Bohai Sea also support our hypothesis that the remaining oil slicks moved northeast along the coast of Hebei Province towards Liaodong Bay.

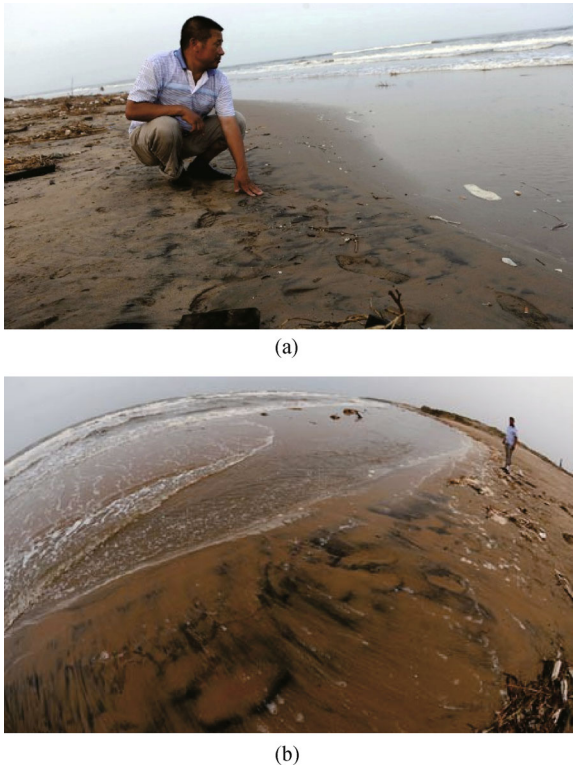

Fig. 5 (a) A Chinese official inspects a beach in northern China's Hebei Province, on July 26, 2011, after an oil sludge washed ashore (Available at http://edition.cnn.com/2012/04/27/world/asia/china-oil-spill/index.html?hpt = hp_bn1). (b) An oil-contaminated beach is seen in Laoting, Hebei Province, on Aug 10, 2011. (Available at http://english.sina.com/china/2011/0811/387980.html).

4 Summary

Many studies have been performed to monitor oil spill trajectories using satellite remote sensing data and model simulations. The investigation on oil spill beaching risk assessment in the coastal regions has become the hot spot after the occurrence of the oil spill, particularly after the BP oil spill event in the Gulf of Mexico. Consequently, the oil spill beaching risk should be given more serious consideration after the Bohai oil spill events in 2011.

In this study, we predicted the oil spill beaching area in the Bohai Sea using GNOME with SAR observed oil spill distribution as initial input. Studies show that the coastal regions along the Hebei Province are at high risk for oil

spill beaching. The oil slicks moved 133 km northward in 12 days. The remaining oil slicks moved northeast towards the Liaodong Bay. However, local field measurements are required to distinguish the sources of the oils. For example, oil spills released from the SZ 36-1 oilfield on July 12, 2011, with spatial coverage of 0.1 m^3 to 0.15 m^3 could also be linked to the observed oil slicks over these regions.

The actual beaching process is more complicated than the results shown here and could be affected by the oil spill cleaning activities. However, the model simulation can capture the basic movement of the oil slicks and is significant for coastal environment conservation and risk management in the Bohai Sea.

Acknowledgements Helpful discussion with Dr. Xiaofeng Li from NOAA is appreciated. This work was supported in part by the National Natural Science Foundation of China (Grant No. 41306194), the Open Fund of Shandong Provincial Key Laboratory of Marine Ecology and Environment & Disaster Prevention and Mitigation (No. 2011001), the Shanghai Municipal Science and Technology Commission (No. 13dz12044000), and the outstanding innovative talent program of Hohai University.

References

Beegle-Krause C J (2003). Advantages of separating the circulation model and trajectory model: GNOME trajectory model used with outside circulation models. Environment Canada Arctic and Marine Oil Spill Program Technical Seminar (AMOP) Proceedings, 26(2): 825–840

Beegle-Krause C J (2005). General NOAA oil modeling environment (GNOME): a new spill trajectory model. In: Proceedings of International Oil Spill Conference, 3277–3283

Cheng Y, Li X, Xu Q, Garcia-Pineda O, Andersen O B, Pichel W G (2011). SAR observation and model tracking of an oil spill event in coastal waters. Mar Pollut Bull, 62(2): 350–363

Cheng Y, Liu B, Li X, Nunziata F, Xu Q, Ding X, Migliaccio M, Pichel W G (2014). Monitoring of oil spill trajectories with COSMO-SkyMed X-Band SAR images and model simulation. IEEE J Sel Topics Appl Earth Observ in Remote Sens, 7(7): 2895–2901

Farzingohar M, Zelina Z I, Yasemi M (2011). Oil spill modeling of diesel and gasoline with GNOME around Rajaee Port of Bandar Abbas. Iran J Fish Sci, 10: 35–46

Ferraro G, Meyer-Roux S, Muellenhoff O, Pavliha M, Svetak J, Tarchi D, Topouzelis K (2009). Long term monitoring of oil spills in European seas. Int J Remote Sens, 30(3): 627–645

Garcia-Pineda O, Zimmer B, Howard M, Pichel W G, Li X, MacDonald I R (2009). Using SAR image to delineate ocean oil slicks with a texture classifying neural network algorithm (TCNNA). Can J Rem Sens, 35(5): 411–421

Guo J, Liu X, Xie Q (2013). Characteristics of the Bohai Sea oil spill and its impact on the Bohai Sea ecosystem. Chin Sci Bull, 58(19): 2276–2281

Hackett B, Comerma E, Daniel P, Ichikawa H (2009). Marine oil pollution prediction. Oceanography (Wash DC), 22(3): 168–175

Hu C, Li X, Pichel W G, Muller-Karger F E (2009). Detection of natural oil slicks in the NW Gulf of Mexico using MODIS imagery. Geophys Res Lett, 36(1 L01604): L01604

Hu C, Müller-Karger F E, Taylor C, Myhre D, Murch B, Odriozola A L, Godoy G (2003). MODIS detects oil spills in Lake Maracaibo, Venezuela. Eos Trans AGU, 84(33): 313–319

Li X, Li C, Yang Z, Pichel W (2013). SAR imaging of ocean surface oil seep trajectories induced by near inertial oscillation. Remote Sens Environ, 130: 182–187

Li X, Zheng W, Pichel W G, Zou C Z, Clemente-Colón P (2007). Coastal katabatic winds imaged by SAR. Geophys Res Lett, 34(3), L03804, doi: 10.1029/2006GL028055

Liu P, Li X, Qu J, Wang W, Zhao C, Pichel W G (2011). Oil spill detection with fully polarimetric UAVSAR data. Mar Pollut Bull, 62 (12): 2611–2618

Martin P J, Barron C N, Smedstad L F, Campbell T J, Wallcraft A J, Rhodes R C, Rowley C, Townsend T L, Carroll S N (2009). User's manual for the Navy Coastal Ocean Model (NCOM) version 4.0, NRL Report NRL/MR/732009-9151

Migliaccio M, Gambardella A, Tranfaglia M (2007). SAR polarimetry to observe oil spills. IEEE Trans Geosci Rem Sens, 45(2): 506–511

Migliaccio M, Nunziata F, Brown C E, Holt B, Li X F, Pichel W, Shimada M (2012). Polarimetric synthetic aperture radar utilized to track oil spills. EOS, 16(93): 161–168

Remyalekshmi R, Hegde A V (2013). Numerical modeling of oil spill movement along north-west coast of India using GNOME. International Journal of Ocean and Climate Systems, 4(1): 75–86

Solberg A H S, Brekke C, Husoy P O (2007). Oil spill detection in radarsat and envisat sar images. IEEE Trans Geosci Rem Sens, 45(3): 746–755

Sun P, Gao Z, Cao L, Wang X, Zhou Q, Zhao Y, Li G (2011). Application of a step-by-step fingerprinting identification method on a spilled oil accident in the Bohai Sea area. J Ocean Univ China, 10 (1): 35–41

Wackerman C, Clemente-Colon P, Pichel W, Li X (2002). A two-scale model to predict C-band VV and HH normalized radar cross section values over the ocean. Can J Rem Sens, 28(3): 367–384

Wang C, Liao M, Li X (2008). Ship detection in SAR image based on the alpha-stable distribution. Sensors, 8(8): 4948–4960

Xu Q, Li X, Wei Y, Tang Z, Cheng Y, Pichel W G (2013). Satellite observations and modeling of oil spill trajectories in the Bohai Sea. Mar Pollut Bull, 71(1−2): 107–116

Xu Q, Lin H, Li X, Zou J, Zheng Q, Pichel W G (2010). Assessment of an analytical model for sea surface wind speed retrieval from space-borne SAR. Int J Remote Sens, 31(4): 993–1008

Xu Q, Xi H, Zhang Y (2010). Marine pollution in water, sediment and biota. In: Ahmed E N, ed. Impact, Monitoring and Management of Environmental Pollution. Hauppauge NY: Nova Science Pub Inc., 157–191

Yang X, Li X, Zheng Q, Gu X, Pichel W G, Li Z (2011). Comparison of ocean-surface winds retrieved from QuikSCAT scatterometer and Radarsat-1 SAR in offshore waters of the U.S. west coast. IEEE Geosci Remote Sens Lett, 8(1): 163–167

Zhang B, Perrie W, Li X, Pichel W G (2011). Mapping sea surface oil slicks using RADARSAT-2 quad-polarization SAR image. Geophys Res Lett, doi: 10.1029/2011GL047013